CLIMA 2016 - proceedings of the 12th REHVA World Congress

volume 10

Heiselberg, Per Kvols

Publication date:
2016

Document Version
Publisher's PDF, also known as Version of record

Link to publication from Aalborg University

Citation for published version (APA):
Heiselberg, P. K. (Ed.) (2016). *CLIMA 2016 - proceedings of the 12th REHVA World Congress: volume 10*. Department of Civil Engineering, Aalborg University.

Numerical study on load shifting strategies for the heating and cooling of an office building considering variable grid conditions

Konstantin Klein[1*], Doreen Kalz[2] and Sebastian Herkel[3]

[#]*Thermal Systems and Buildings, Fraunhofer-Institute for Solar Energy Systems ISE*

Heidenhofstr. 2, 79110 Freiburg

[1]konstantin.klein@ise.fraunhofer.de

[2]doreen.kalz@ise.fraunhofer.de

[3]sebastian.herkel@ise.fraunhofer.de

Abstract

In this simulation study, the load shifting potential of a plus-energy office building with local PV generation, a ground-coupled heat pump and TABS using the heating and cooling system is discussed. The evaluated load shifting strategy uses the building mass as a thermal storage by rescheduling the delivery of thermal energy to the zones, based on the availability of local PV generation and the fraction of wind and PV in the public grid. It is implemented as a co-simulation of Dymola (for simulation of the full system) and Python (for the load shifting algorithm and test of comfort criteria using a functional mock-up unit (FMU) of the building).

Using the presented strategy, self-consumption and autonomy of the locally produced electricity can be increased by $3\%_{abs}$ and the grid support coefficient GSC_{rel} of the heat pump can be increased from -11 to +58 while maintaining thermal comfort. Between spring and autumn, the load shifting potential of the heat pump is limited due to low heating and cooling demand. It can be increased by a factor of 2-3 if the comfort requirements are relayed by a soft constraint. Load shifting decreases the efficiency of the heating and cooling system by 2.8%.

Keywords – load shifting ; demand response ; heat pumps ; self-consumption; building ; simulation

1. Introduction

As part of the Energy transition, the German federal government plans to cover at least 80% of its electricity consumption with renewables by the year 2050 [1], mostly by wind and PV plants. Due to the volatile nature of wind and PV power, the relative availability of electricity in the German energy system will be subject to strong and increasing temporal fluctuations.

Demand flexibilization has been identified as one key measure to reduce negative effects of a high share of fluctuating renewables, such as grid overload (congestion) and required shutoff of renewable electricity production (curtailment) [2]. Buildings using heat pumps, compression chillers or CHP units can contribute to demand flexibilization by adapting the operation of local heating and cooling energy production according to the relative availability of electricity in the grid and store the thermal energy. Previous studies [3-4] suggest that buildings with heat pumps are generally well suited for load shifting.

The current paper is a continuation of the work presented in [5]. It quantifies the load shifting potential of a generic, newly constructed European net-zero energy office building with local PV generation, thermally activated building systems (TABS) and a ground-coupled heat pump used for heating and cooling, using the building mass as a thermal storage. The control strategy applied is based on a load-shifting algorithm which maximizes the use of locally produced electricity and grid electricity with a high share of wind and PV. As compared to [5], the algorithm has been extended and refined in several aspects, most notably in that it checks and ensures that the shifted heat delivery complies with thermal comfort requirements (EN 15251:2012-12) to the zone using a functional mock-up unit (FMU) of the building model.

The main research questions addressed in this study are (i) how much heat (and, thus, electricity) can be shifted and stored in a typical office building with TABS, (ii) how load shifting potential varies in the course of the year and (iii) how tolerances for thermal room comfort and the grid priority signal affect the load shifting potential of the building.

2. Evaluation criteria

2.1 In this study, *grid support* is understood as a measure of how well a consumer's electricity consumption profile coincides with the availability of electricity, which is assessed using a grid-based reference quantity, e.g. the stock electricity price or the fraction of wind and PV in the electricity mix.

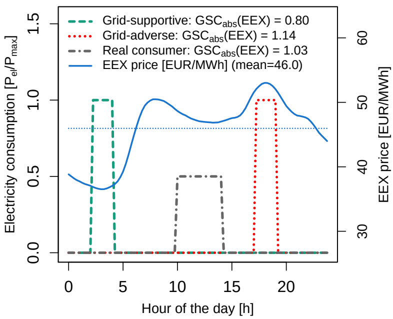

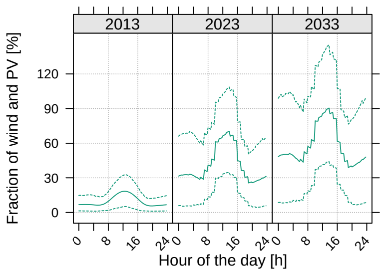

Fig. 1 Left: Grid-supportive, grid-adverse, and uncontrolled consumption behavior during one typical day of operation, using the EEX price as a grid-based reference quantity. Right: Fraction of wind and PV in the German electricity mix in 2013, 2023 and 2033.

Consumption profiles which provide a high level of grid support are referred to as *grid-supportive*, whereas unfavorable characteristics are labeled *grid-adverse*.

In order to quantify grid supportive operation of buildings, the Grid Support Coefficients GSC_{abs} and GSC_{rel} proposed in [6] are used. GSC_{abs} "weights" the electricity consumption profile with a time-resolved reference. GSC_{rel} relates GSC_{abs} to the worst and best achievable values on a scale of -100 to 100 in order to increase the comparability of the results. Referring to the numerical example illustrated in the left-hand diagram in Fig. 1, a GSC_{abs}(EEX) value of 1.14 means that electricity is, on weighted average, consumed from the grid when the stock electricity price is 14% above average, which is grid-adverse.

2.2 Comfort

Thermal comfort is evaluated based on European Standard EN 15251:2012-12. As recommended for office buildings, comfort class with the defined upper and lower temperature limits II is used. Accordingly, interior temperatures of 22°C ± 2 K are tolerable in the heating season and interior temperatures of 24.5°C ± 1.5 K are tolerable in the cooling season. In this contribution, we understand exceedances, measured in Kelvin hours (Kh), as deviations of the operative room temperature from the defined comfort tolerance band while the zone is occupied.

3. Modeling

3.1 Building

The building studied is a generic 6-storey office building located in Mannheim, Germany. It is divisible into eight rows of geometrically identical three-zone-cells. The rows in the center and at the West end of the building consist of one north-facing two-person office, one south-facing two-person office, as well as a connecting corridor. The zones at the East end of the buildings contain the staircase, elevator, lavatories and a small kitchen. The building has a total floor area of 2,433.6 m^2. Its building shell properties comply with the requirements of the building code (EnEV 2014) for non-residential buildings. The building is equipped with a total of 422 Schott Perform Poly 245 PV panels mounted on the Southern, Eastern and Western façade as well as the roof, as indicated in blue shade in Fig. 2. The offices are partially occupied during workdays between 7 a.m. and 6 p.m. with six full-occupancy hours per day. The heat gains from people and appliances are 70 W/person and 100 W/person, respectively, in compliance with DIN-V 18599:2011-12. It is assumed that a continuous lighting controller keeps the illuminance on the working surfaces at or above 300 lux.

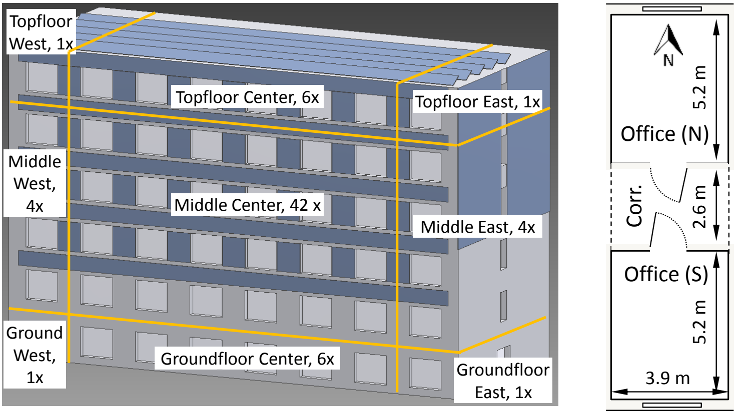

Fig. 2 Illustration of building with indication of the 9 defined segments of the detailed model (left) and floor plan of one three-zone segment (right)

Table 1 Physical and geometrical properties of the building

Thermal properties	Value	Unit	Offices properties	Value	Unit
U-value, ext. wall	0.24	W/m^2K	Zone width	3.9	m
U-value, roof	0.2	W/m^2K	Zone depth	5.2	m
U-value, baseplate	0.3	W/m^2K	Zone height	3	m
U-value, windows	1.0	W/m^2K	window area (glazing)	4.68	m^2
g-value, windows	0.58		air exchange, occupancy	30	m^3/ Pers./h
shading factor	0.4	-	infiltration rate	0.3	h^{-1}

The model for each zone is based on a 5R2C resistor-capacitor-model in compliance with the modeling standards of EN ISO 13790:2008-09. The heat exchange via TABS is modeled using a slab model from the Modelica Buildings library, which is thermally connected to the zone at the surface and air nodes. The concrete slab is discretized in 10 layers to get a close representation of the thermodynamic behavior of the building mass.

In the first step, the considered building is modeled as a detailed white-box model using 9 different types of segments (e.g. “Middle Center”, see Fig. 2), each of them consisting of a North office, a South office and a corridor.

This white-box model is not practicable for the research question at hand due to its high number of states and, consequently, long simulation times (approx. 36 hours for one annual simulation, including hydraulics and control). Therefore, a simplified, significantly faster grey-box model is calibrated based on the simulated thermal energy consumption of the detailed building model. The simplified model contains only the “Middle Center” segment of the detailed building model, extended by a multiplication factor and two thermal conductances, which are located between each office’s air node and the ambient air, representing the additional heat loss through the roof and baseplate as well as the eastern and western façade of the building. The values for the multiplication factor and the two conductances are determined in a parameter-fit optimization using GenOpt. The relative error between the heat consumption of the detailed and simplified models is below 2% while the simulation speed is 20-25 times faster.

3.3 Heat pump and hydraulic system

The heat pump model is an equation-based model, which computes the COP from the evaporator and condensor temperatures based on the Carnot COP and Carnot efficiency factor. The latter is taken from the experimental measurements of Pärisch [7] as a function of the temperature lift of the heat pump. The buffer tank model is taken from the Annex 60 library [8]. The hydraulic system includes separate hydraulic circuits for the North and South office zones such that different supply temperatures can be chosen.

4. Control and load shifting strategies

4.1 Conventional controller

In the reference case, the circulation pumps are operated continuously during the heating and cooling seasons with a specific mass flow rate of 15 $kg/(m^2 \cdot h)$. Linear heating and cooling curves (offset and slope) as well as heating and cooling limit temperatures are optimized using dynamic simulations such that the annual thermal energy use and deviations of the room temperature from the defined tolerance range are minimized. This is done separately for the north-facing and the south-facing office zones.

4.2 Load shifting strategy

As the first part of the toolchain, (see Fig. 3), an annual simulation of the full system with conventional control is conducted using Dymola (sim1). The heat delivery to the zones is shifted in Python in the steps (1-8). The modified head delivery schedules are then applied in the second full system simulation (sim2). In order to transmit the same thermal energy in shorter time intervals, the heating and cooling curves are shifted up and down by 3 K, respectively.

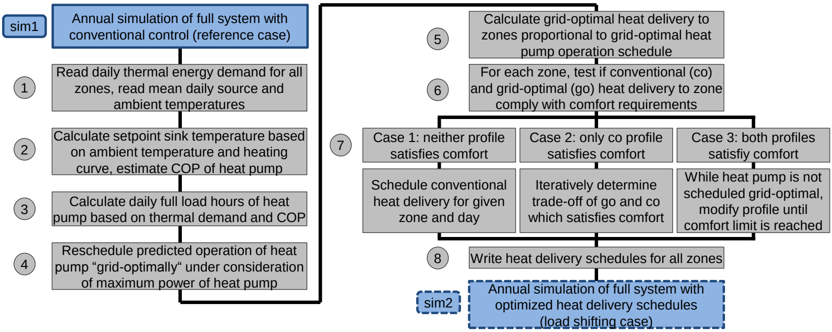

Fig. 3 Procedure of load shifting script. Steps "sim1" and "sim2" are executed in Dymola 2015FD01, steps (1-8) are executed in Python and PyFMI.

In the first step of the load shifting in Python, the daily heating and cooling energy demand per zone is determined. Based on the source and sink temperatures for the given day, the efficiency (COP) of the heat pump is predicted (2) and the number of full operation hours of the heat pump is determined (3). The operation trajectory of the heat pump is rescheduled "grid-optimally". This means that any PV production that exceeds fixed electrical loads of the building is utilized and that the remaining electricity demand of the heat pump is covered with grid electricity with the highest possible fraction of wind and PV (4). The grid-optimal delivery trajectory to the zones is calculated proportionally to the grid-optimized operation trajectory of the heat pump, such that the thermal demand of the zone is covered (5). Following this, the grid-optimal and conventional heat delivery trajectories are tested for compliance with the comfort requirements (6), using a low-order FMU model of the building zone via PyFMI [9]. Three cases are distinguished (7): if none of the profiles is comfort-compliant, e.g. the room temperatures leave the allowed range (Case 1), the conventional heat supply profile to the given zone is used (see chapter 4.1). In case only the conventional profile meets the comfort requirements (Case 2), a trade-off between the conventional and grid-optimal profile is determined, using an algorithm which iteratively assimilates the grid-optimal profile and the conventional profile, starting with the time steps that affect grid support the least, until the comfort criteria are met. If the grid-optimal profile meets the comfort requirements, e.g. deviation from the room temperature tolerance band (Case 3), the grid-optimal profile is optimized further using an algorithm which iteratively shifts thermal energy from the most grid-adverse hours to the most grid-supportive hours, limited by the predicted compressor power of the heat pump and the maximum charging power of the TABS (about 50 W/m^2).

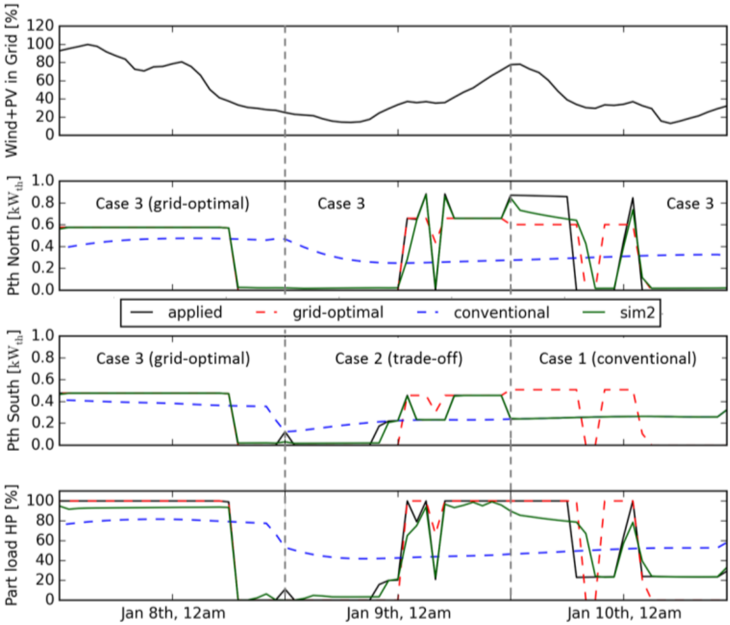

Fig. 4 Fraction of wind and PV in the grid [%], heat delivery trajectories for the North and South zones, and part load ratio of the heat pump for three days in January. Blue and red lines: conventional (chap. 4.1) and grid-optimal (chap. 4,2) trajectories; solid black lines: final trajectories determined by the algorithm. Green lines: actual behavior in the full system simulation (sim2).

Fig. 4 shows the performance of the algorithm for three days in January. During that period, fixed electric loads exceed the local PV production; thus, the algorithm aims to shift heating to times with a high fraction of wind and PV in the electricity mix. In the southern zone, the grid-optimal profile satisfies comfort during Jan 8th (Case 3), whereas a trade-off profile has to be determined during Jan 9th (Case 2) and the conventional profile is applied during Jan 10th (Case 1). In the North zone, the grid-optimal profile complies with comfort requirements during all three days. System performance in the annual full system simulation (sim2, green lines) is similar to the behavior predicted by the algorithm (black lines).

5. Results

The local PV system generates 66.4 MWh$_{el}$ annually, which equals 115% of the annual electricity consumption (heat pump, pumps, lighting, appliances and plug loads) of the building. However, there is a large seasonal mismatch between electricity demand and local PV generation (Fig. 5).

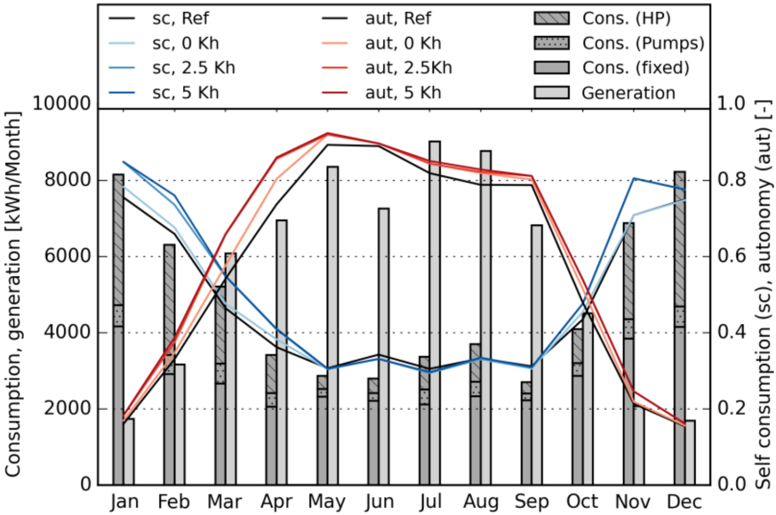

Fig. 3 Monthly analysis of the electric loads of the building (shiftable and non-shiftable)

In winter (January-February), shiftable loads (i.e. heat pump and pumps) account for ca. 50% of the total electricity consumption. However, the PV generation only amounts to one fifth of the consumption. Therefore, the algorithm mainly increases the wind and PV content of the electricity consumed from the grid. In the months May-June and September, there is little to no heating or cooling demand; therefore, the load shifting potential is very limited. In peak summer (July-August), the load shifting potential is only slightly higher. This is attributable to the high efficiency of the ground-coupled heat pump in combination with TABS in cooling mode, which results in small heat pump compressor loads.

Self-consumption and autonomy can be further increased if soft constraints on the comfort boundaries are introduced. In this case, small exceedences of the tolerated room temperature are allowed within the the comfort evaluation in steps (6-7) of the load shifting algorithm. Note that in this case, it is no longer granted that the building complies with the comfort requirements of DIN EN ISO 15251, Class II. These small exceedences typically occur in the beginning of occupancy hours (8 a.m.), when the operative room temperature is slightly below 20 °C. For example, if 2.5 Kh of discomfort per day and zone are allowed in the algorithm (variant “2.5 Kh” in Fig. 5), annual self-consumption is increased from 39.6% to 41.7% and annual autonomy is increased from 45.5% to 49.3%.

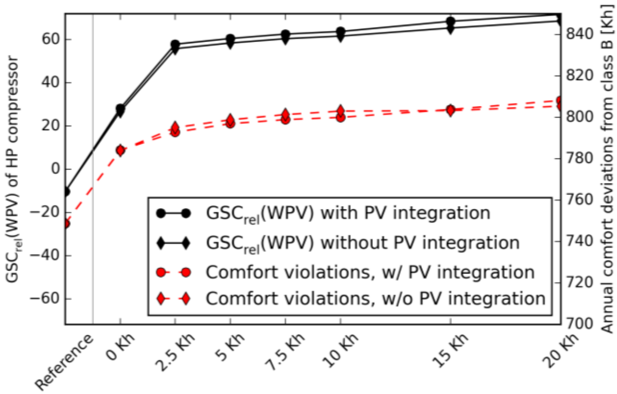

Fig. 6 Relative Grid support coefficient (GSC_{rel}) of the heat pump and annual comfort violations depending on the comfort tolerance and the integration of local PV production

The relative grid support coefficient of the heat pump (GSC_{rel}, worst value: -100, best value: +100) can be improved from -11 (“Reference”) to +28 without changing the comfort requirements (“0 Kh”, Fig. 6). In the variant with the smallest relaxation of the comfort constraint (2,5 Kh”), GSC_{rel} is increased to +58. If the comfort constraint is relaxed further (variants “5 Kh” to ”20 Kh”), GSC_{rel} is improved marginally to about +70. The actual occurring annual exceedances of the room temperature are in all cases less than 8% higher than in the reference case (conventional operation).

If the availability of excessive local PV production is ignored (variants ‘without PV integration’ in Fig. 6) or if a different grid signal, e.g. the residual load of Germany, is used to prioritize operating times for the heat pump (not shown), neither grid support nor the resulting exceedances of the room temperature are strongly affected. This is because for the chosen grid reference year (2023), the periods with a high local PV production coincide well with the periods with a high share of renewables in the grid and a low residual load, which is not yet the case today (as of 2013, see [6]). It can be concluded that within a time frame of less than 10 years, there will be no major conflict between a preferred usage of local PV production and a highly grid-supportive operation of the heating and cooling system.

In terms of energy efficiency, load shifting reduces the Seasonal performance factor (SPF) of the heat pump as a consequence of a higher heating curve and a lower cooling curve, and saves pump electricity due to shorter operation times of the pumps. The combined power consumption of heat pump and circulations pumps is increased by 2.8% due to load shifting.

6. Conclusion and outlook

Using a plus-energy office building with TABS and a ground-coupled heat pump as an example, it was shown that the presented load-shifting strategy leads to a more grid-supportive heat pump operation while maintaining comfort. Putting a soft constraint on comfort requirements increases the load shifting potential. For the given system, the big seasonal mismatch between local electricity generation and demand of the heat pump limit the load shifting potential.

The authors intend to adapt and apply the presented operation strategy to different technologies, e.g. CHP units as heat generators, different heat delivery systems, and building insulation standards, in order to compare the load shifting potential for different types of buildings and supply concepts.

Furthermore, the applied load shifting strategy will be extended so that it also utilizes the hot and cold water storages, batteries, and potentially different types of heat and cold generators ("fuel switch") for load shifting in order to determine which "flexibility option" within the building provides the highest and most usable flexibility.

Acknowledgment

The study was carried out in the framework of the project "Netzreaktive Gebäude" (www.netzreaktivegebaeude.de). The authors gratefully acknowledge the financial support by the German Federal Ministry of Economics and Energy (project code: 03ET1111A).

References

[1] Federal Government of Germany, Der Weg zur Energie der Zukunft – sicher, bezahlbar und umweltfreundlich [in German; translated title: The Way to future Energy – safe, affordable and ecological], 2011: Berlin.
[2] Lund PD, Lindgren J, Mikkola J, Salpakari J. Review of energy system flexibility measures to enable high levels of variable renewable electricity. Renew Sustain Energy Rev 2015;45(May):785–807. http://dx.doi.org/10.1016/jrser.2015.01.057.
[3] deConinck, R: Grey-Box Based Optimal Control for Thermal Systems in Buildings - Unlocking Energy Efficiency and Flexibility. PhD thesis, KU Leuven, 2015.
[4] Reynders, G.: Quantifying the impact of building design on the potential of structural storage for active demand response in residential buildings. PhD thesis, KU Leuven, 2015.
[5] Klein, K., Kalz, D., Herkel, S.: Grid impact of a net-zero energy building with BiPV dusing different energy management strategies. CISBAT 2015, 9.-11. September 2015, Lausanne
[6] K. Klein, R. Langner, D. Kalz, S. Herkel, H.-M. Henning: Grid support coefficients for electricity-based heating and cooling and field data analysis of present-day installations in Germany. Applied Energy 162 (2016), pp. 853-867, http://dx.doi.org/10.1016/j.apenergy.2015.10.107
[7] Pärisch, P., Mercker, O., et al.: Investiations and model validation of a ground-coupled heat pump for the combination with solar collectors. Applied Thermal Engineering 62 (2014), pp. 375-381. http://dx.doi.org/10.1016/j.applthermaleng.2013.09.016
[8] Modelica Annex60 library. https://github.com/iea-annex60/modelica-annex60
[9] PyFMI: A package for working with dynamic models compliant with the Functional Mock-Up Interface standard. https://pypi.python.org/pypi/PyFMI